

INFLUENCE OF INCLINATIONS APPLIED TO RIBS ON THE SOLIDIFICATION OF CAST PARTS

**Aurel CRIȘAN, Diana ȚUȚUIANU,
Tibor BEDÓ, Ioan CIOBANU**

„Transilvania” University of Brașov,
Faculty of Materials Science and Engineering
email: crisan.a@unitbv.ro

ABSTRACT

The inclinations and corner radii applied to ribs are designed for enhancing both stiffness and aesthetics. The presence of inclinations applied to ribs modifies the conditions of heat transmission and implicitly the solidification of the alloy in the joining area of the rib to the part wall. This is highlighted by changing the radius of circles inscribed in the wall - rib joining area. The diameter of the circles inscribed in this area is greater than of those in rest of the part wall. This leads to the assumption that the solidification of the alloy in the wall-rib joining area is slowed. The paper presents the results of a study concerning the influence of inclinations applied to ribs on the duration of cast part solidification and on the position of the hot spots. The study was conducted by computer simulation of solidification. The results have revealed that for certain limits this influence is negligible. Instead, in case of large inclinations, solidification time increases considerably. The limits for which the influence of inclinations applied to ribs becomes significant are determined.

KEYWORDS: rib inclination, cast part solidification, hot spots

1. Introduction

While representing the technological elements required by the designer or manufacturing engineer, ribs, casting slopes and corner radii of the cast parts also have an aesthetic function. Generally ribs have the role of stiffening the walls of the cast parts.

These technological elements (ribs, slopes, corner radii) influence the solidification of cast parts.

Ribs determine a local thickening of parts in the rib – part wall joining area, as highlighted by the local increase of the circle radii inscribed in the part perimeter, as shown in Figure 1.

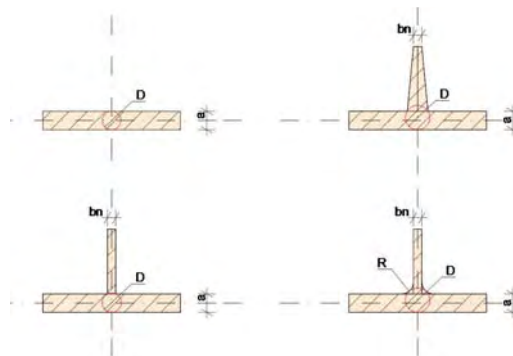


Fig. 1. Influence of rib thickness, casting slopes and corner radii on the diameter of the circle inscribed in the contour of the cast parts.

Consequently it is to be expected that these technological elements determine a local increase of solidification time and hence the generation of hot spots, causing on their turn solidification-specific

defects (porosity, shrinkholes, cracks, etc.). The paper presents the results of a study on the influence of inclinations applied to ribs on the solidification of cast parts, and thus on the tendency of defect generation caused by solidification. The aim is to establish the magnitude of this influence and the opportunity of

prevention measures. Research was conducted by computer aided simulation of the solidification process.

The dedicated „Sim-3D” software, developed at the Faculty of Materials Science and Engineering of the Transilvania University of Brasov was used.

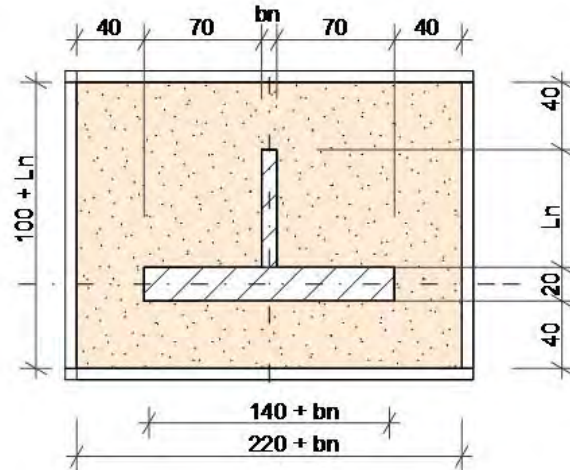


Fig. 2. Geometry and dimensions of the part and mould.

2. Influence of rib inclination on cast part solidification

It has been conducted a study on the influence of rib lateral face inclination on the solidification of cast parts. The study was conducted for a part of 20 mm thickness. Figure 2 shows the geometry and the dimensions of the cast parts and the mould involved in the study. Rib length was of $L_n = 60$ mm. The study was conducted for rib widths of $b_n = 3$ mm, 5 mm and 15 mm Rib inclination varied between $t\alpha = 0$ and $t\alpha$

$= 3/20$. The rib lateral face inclination was applied by rib wall thickening. The part was cast from eutectic cast iron in a silica sand mould.

Computer simulation was used to study the influence of the rib lateral wall inclination on the position of the hot spots, solidification time, and temperature variation of the solidified fraction in the hot spots.

Table 1 features the thermo-physical characteristics of the alloy and the mould used for simulation.

Table 1. Values of the quantities used for simulation of solidification

No.	Parameter	Physical symbol	Measure unit	Value
1	Mesh width of mould dividing	Δ	m	0.001
2	Time interval	τ	s	0.02
3	Environment temperature for the exterior of the mould	T_{ex}	$^{\circ}C$	20
4	Thermal exchange coefficient of mould-exterior environment	α_{ex}	$W \cdot m^{-2} \cdot K^{-1}$	10.0
5	Solidus temperature of the cast alloy	T_{sme}	$^{\circ}C$	1150
6	Thermal conductivity coefficient of the mould	λ_{sfo}	$W \cdot m^{-1} \cdot K^{-1}$	0.85
7	Thermal conductivity coefficient of the solidified alloy	λ_{sme}	$W \cdot m^{-1} \cdot K^{-1}$	40
8	Thermal conductivity coefficient of the liquid alloy	λ_{lme}	$W \cdot m^{-1} \cdot K^{-1}$	30
9	Specific heat of the mould	C_{sfo}	$J \cdot kg^{-1} \cdot K^{-1}$	1170
10	Specific heat of the liquid cast iron	C_{lme}	$J \cdot kg^{-1} \cdot K^{-1}$	850
11	Specific heat of the solid cast iron	C_{sme}	$J \cdot kg^{-1} \cdot K^{-1}$	750
12	Mould density	ρ_{fo}	$kg \cdot m^{-3}$	1550
13	Alloy density	ρ_{me}	$kg \cdot m^{-3}$	6700
14	Specific latent heat of the cast alloy	L_{me}	$J \cdot kg^{-1}$	250000
15	Initial temperature of the mould	T_{0fo}	$^{\circ}C$	20
16	Initial temperature of the cast alloy	T_{0me}	$^{\circ}C$	1350



Figures 3 ÷ 14 show the distribution of isotherms in the cast part and in the mould at the solidification time of the hot spots in a number of the studied cases. Tables 2 ÷ 4 feature the coordinates of the hot spots and their corresponding solidification times. The coordinates of the hot spots are given in relation to a frame of reference corresponding to the symmetry

axis of the cast part and of the rib, as shown in Figure 15.

Figure 16 presents the influence of rib wall inclination of the solidification time of the hot spots. Figures 17 ÷ 20 feature the variation curves of temperature and the solid fraction in the hot spots for several of the studied cases.

Table 2. Coordinates of the hot spots and solidification time versus rib wall inclination (ribs of thickness $b_n = 3$ mm and length $L_n = 60$ mm).

No.	Rib inclination	No. of hot spots	Coordinates of hot spots	Solidification time
Symbol	$\text{tg } \alpha$	N_n	(x,y)	t_{sol}
u.m.	-	-	(mm,mm)	s
1	0	2	(-20.0; -0.5) and (+20.0; -0.5)	233.08
2	1/60	2	(-20.0; -0.5) and (+20.0; -0.5)	264.94
3	2/60	2	(-19.0; +0.5) and (+19.0; +0.5)	270.16
4	3/60	2	(-18.0; +0.5) and (+18.0; +0.5)	277.12
5	4/60	2	(-16.0; +0.5) and (+16.0; +0.5)	284.98
6	5/60	2	(-15.0; +0.5) and (+15.0; +0.5)	293.92
7	9/60	1	(0; -0.5)	340.36

Table 3. Coordinates of the hot spots and solidification time versus rib wall inclination (ribs of thickness $b_n = 5$ mm and length $L_n = 60$ mm).

No.	Rib inclination	No. of hot spots	Coordinates of hot spots	Solidification time
Symbol	$\text{tg } \alpha$	N_n	(x,y)	t_{sol}
u.m.	-	-	(mm,mm)	s
1	0	2	(-19.0; +0.5) and (+19.0; +0.5)	271.58
2	1/60	2	(-18.0; +0.5) and (+18.0; +0.5)	277.42
3	2/60	2	(-17.0; +0.5) and (+17.0; +0.5)	284.88
4	3/60	2	(-15.0; +0.5) and (+15.0; +0.5)	193.44
5	4/60	2	(-13.0; +0.5) and (+13.0; +0.5)	302.62
6	5/60	2	(-12.0; +0.5) and (+12.0; +0.5)	312.64
7	9/60	1	(0; +1.5)	366.12

Table 4. Coordinates of the hot spots and solidification time versus rib wall inclination (ribs of thickness $b_n = 15$ mm and length $L_n = 60$ mm).

No.	Rib inclination	No. of hot spots	Coordinates of hot spots	Solidification time
Symbol	$\text{tg } \alpha$	N_n	(x,y)	t_{sol}
u.m.	-	-	(mm,mm)	s
1	0	1	(0; +1.5)	365.30
2	1/60	1	(0; +2.5)	379.58
3	2/60	1	(0; +2.5)	393.66
4	3/60	1	(0; +3.5)	407.58
5	4/60	1	(0; +4.5)	421.42
6	5/60	1	(0; +5.5)	435.22
7	9/60	1	(0; +9.5)	490.94

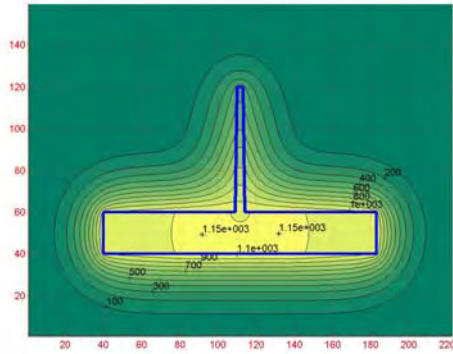


Fig. 3. Distribution of isotherms at the end of solidification for a rib of inclination $\text{tg } \alpha = 1/60$ and thickness $b_n = 3 \text{ mm}$ (at the moment of solidification $t_{\text{sol}}=264.94\text{s}$).

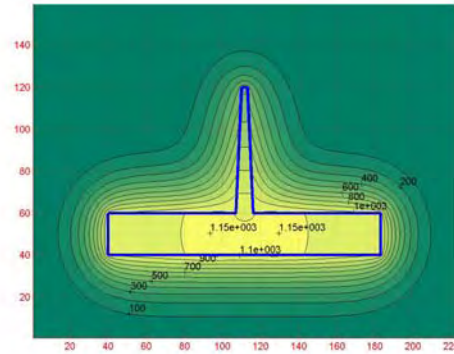


Fig. 4. Distribution of isotherms at the end of solidification for a rib of inclination $\text{tg } \alpha = 3/60$ and thickness $b_n = 3 \text{ mm}$ (at the moment of solidification $t_{\text{sol}}=277.12\text{s}$).

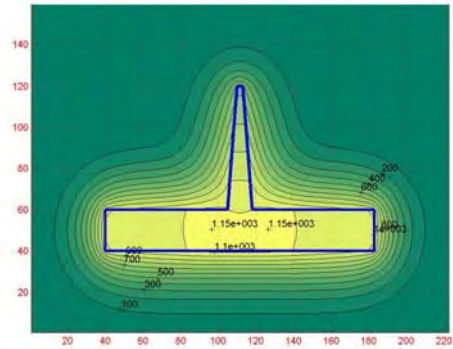


Fig. 5. Distribution of isotherms at the end of solidification for a rib of inclination $\text{tg } \alpha = 5/60$ and thickness $b_n = 3 \text{ mm}$ (at the moment of solidification $t_{\text{sol}}=293.92\text{s}$).

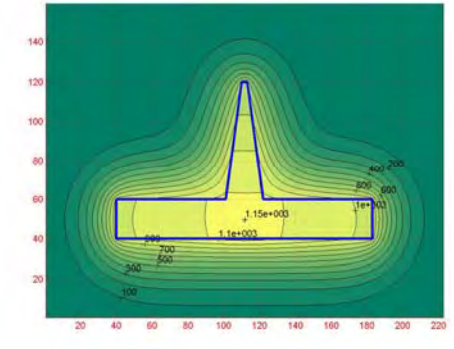


Fig. 6. Distribution of isotherms at the end of solidification for a rib of inclination $\text{tg } \alpha = 9/60$ and thickness $b_n = 3 \text{ mm}$ (at the moment of solidification $t_{\text{sol}}=340.36\text{s}$).

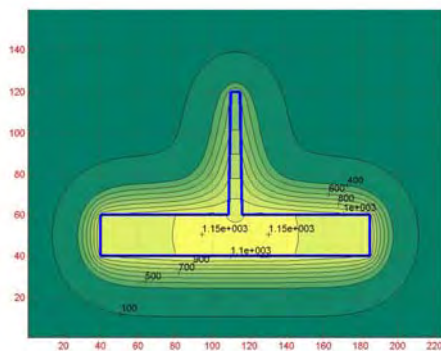


Fig. 7. Distribution of isotherms at the end of solidification for a rib of inclination $\text{tg } \alpha = 1/60$ and thickness $b_n = 5 \text{ mm}$ (at the moment of solidification $t_{\text{sol}}=277.42\text{s}$).

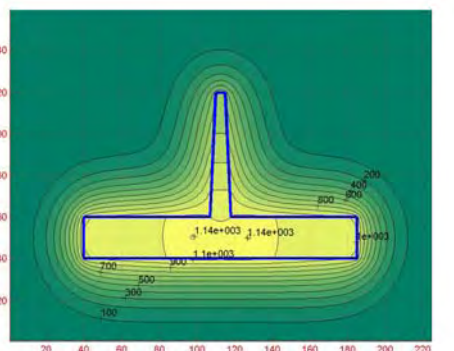


Fig. 8. Distribution of isotherms at the end of solidification for a rib of inclination $\text{tg } \alpha = 3/60$ and thickness $b_n = 5 \text{ mm}$ (at the moment of solidification $t_{\text{sol}}=193.44\text{s}$).

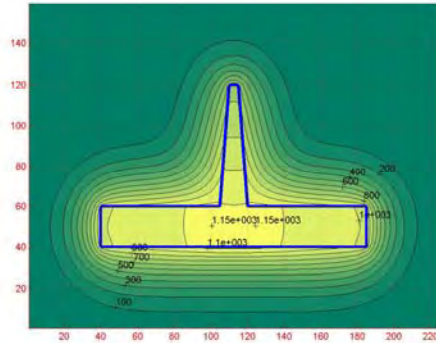


Fig. 9. Distribution of isotherms at the end of solidification for a rib of inclination $\tan \alpha = 5/60$ and thickness $b_n = 5$ mm (at the moment of solidification $t_{sol} = 312.64s$).

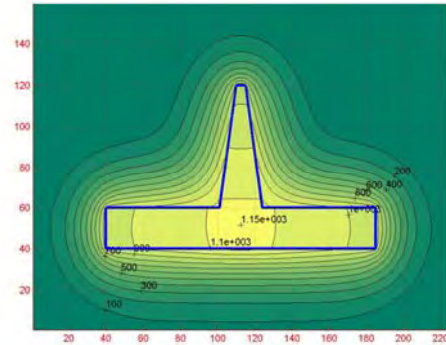


Fig. 10. Distribution of isotherms at the end of solidification for a rib of inclination $\tan \alpha = 9/60$ and thickness $b_n = 5$ mm (at the moment of solidification $t_{sol} = 366.12s$).

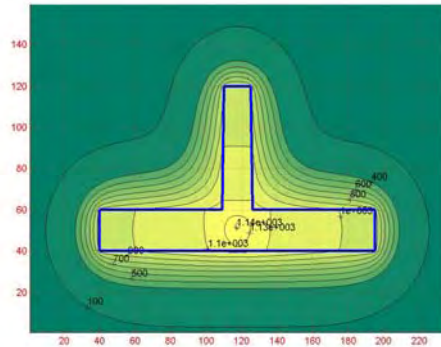


Fig. 11. Distribution of isotherms at the end of solidification for a rib of inclination $\tan \alpha = 1/60$ and thickness $b_n = 15$ mm (at the moment of solidification $t_{sol} = 379.58s$).

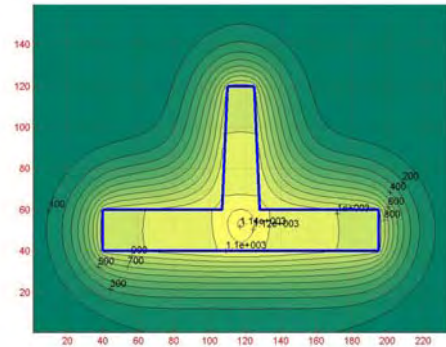


Fig. 12. Distribution of isotherms at the end of solidification for a rib of inclination $\tan \alpha = 3/60$ and thickness $b_n = 15$ mm (at the moment of solidification $t_{sol} = 407.58s$).

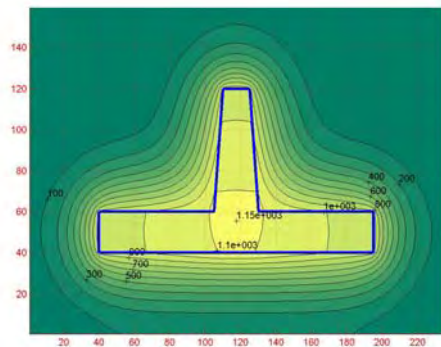


Fig. 13. Distribution of isotherms at the end of solidification for a rib of inclination $\tan \alpha = 5/60$ and thickness $b_n = 15$ mm (at the moment of solidification $t_{sol} = 435.22s$).

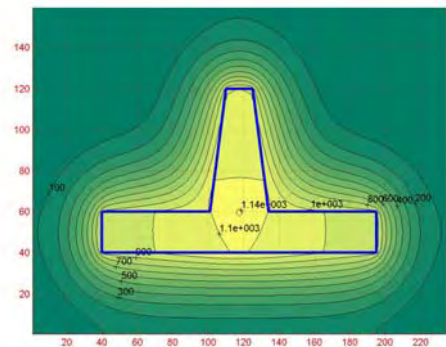


Fig. 14. Distribution of isotherms at the end of solidification for a rib of inclination $\tan \alpha = 9/60$ and thickness $b_n = 15$ mm (at the moment of solidification $t_{sol} = 490.94s$).

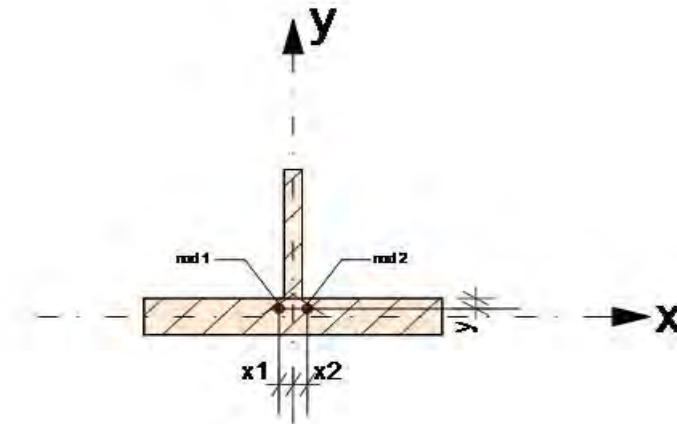


Fig. 15. Coordinates of the hot spots.

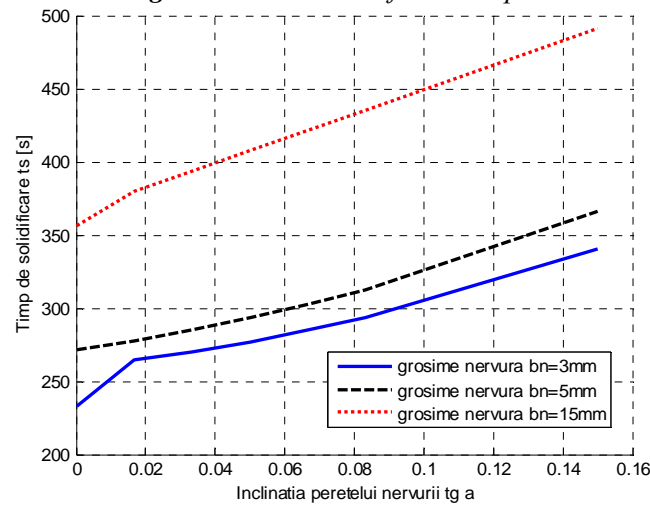


Fig. 16. The influence of rib inclination ($tg \alpha$) on solidification time (part thickness $a = 20mm$, inclinations by increasing rib wall thickness) (t_s = solidification time, $tg \alpha$ = rib wall inclination, b_n = rib thickness).

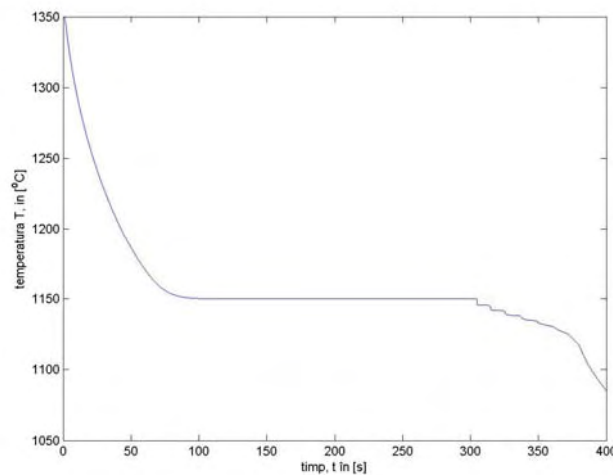


Fig. 17. Temperature variation in the hot spot (coordinates $x = 0 mm$, $y = 2.5 mm$), part with a rib of $b_n = 15 mm$ and inclination $tg \alpha = 1/60$ (T = temperature; t = time).

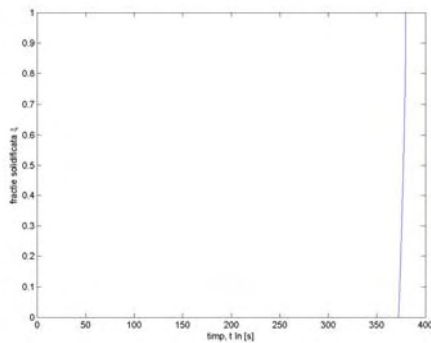


Fig. 18. Variation of the solid fraction in the hot spot during solidification (coordinates $x = 0$ mm, $y = 2.5$ mm), part with a rib of $b_n = 15$ mm and inclination $\text{tg } \alpha = 1/60$ ($\zeta =$ solid fraction).

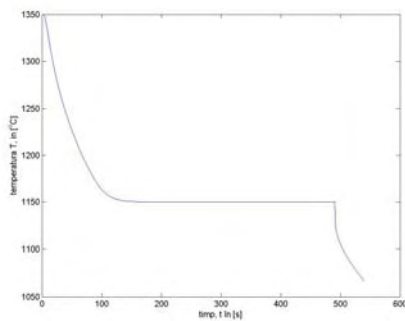


Fig. 19. Temperature variation in the hot spot (coordinates $x = 0$ mm, $y = 9.5$ mm), part with a rib of $b_n = 15$ mm and inclination $\text{tg } \alpha = 9/60$ ($T =$ temperature; $t =$ time).

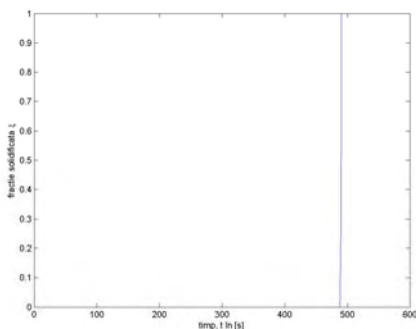


Fig. 20. Variation of the solid fraction in the hot spot (coordinates $x = 0$ mm, $y = 9.5$ mm), part with a rib of $b_n = 15$ mm and inclination $\text{tg } \alpha = 9/60$. ($\zeta =$ solid fraction).

3. Conclusions

The following conclusions are yielded by the results of this study:

- in the case of ribs significantly thinner than the part wall ($b_n = 3$ mm; $b_n = 5$ mm) and for small inclinations of the lateral walls ($\text{tg } \alpha = 1/60 \div 6/60$) the cooling effect of the rib is maintained; two hot spots are generated in the part wall, symmetrical in relation to the rib axis;

- with an increasing inclination of the rib lateral walls the two hot spots move closer to the rib axis, and for an inclination of $\text{tg } \alpha = 9/60$ the two hot spots merge in a single one located on the rib axis (figure 6 and 10);

- in the case of ribs of thickness exceeding $b_n = 15$ mm, even for small inclinations a single hot spot is generated in the cast part, located on the symmetry axis of the part; with an increasing inclination the hot spot slightly moving along the y-axis (moving away from the part wall axis towards the rib);

- the solidification time of the hot spots increases to a relatively high degree in relation to the increase of rib lateral wall inclination; in the studied cases (ribs of thicknesses 3; 5; 15 mm), an increase of inclination from $\text{tg } \alpha = 0$ to $\text{tg } \alpha = 9/60$ determines an increase of solidification time by about 50%.

References

- [1]. Ciobanu I., Monescu V., Munteanu S. I., Crișan A. – *Simularea 3D a solidificării pieselor turnate*, Editura Universității "Transilvania" din Brașov, Brașov, Ro, 2010, ISBN 978-973-598-678-0.
- [2]. Ciobanu I., Țuțuianu Diana – *Estetica, element valoric al pieselor turnate*, Metalurgia, no. 1, pag. 3-8, ISSN 0461/9579.
- [3]. Ciobanu, I., Mașniță, M., Monescu, V. *Cercetări privind solidificarea pieselor cu secțiune "T"*, Metalurgia, nr.13, 2006.
- [4]. Mașniță M. – *Cercetări privind influența unor factori tehnologici și constructivi asupra solidificării pieselor turnate*, Teză de doctorat, Universitatea Transilvania din Brașov, 2007.
- [5]. Țuțuianu Diana, Ciobanu I. – *Considerații privind implicațiile tehnologice și estetice ale înclinațiilor de turnare și ale razelor de racordare în cazul pieselor turnate*, Sesiunea de comunicări științifice cu participare internațională Terra Dacică - România mileniului trei. Acad. Forțelor aeriene Henri Coandă Brasov, 5-6 mai 2006, An VII, nr.1, CD - ISSN 1453 – 0139.
- [6]. Zirbo G., Ciobanu I. – *Tehnologia turnării*, vol 1 & 2, Institutul Politehnic Cluj – Napoca, 1989.